

3. P. Sarda and D. Graham, *ibid.* **97**, 268 (1990).
 4. T. Staudacher *et al.*, *ibid.* **96**, 119 (1989).
 5. M. Javoy and F. Pineau, *ibid.* **107**, 598 (1991); F. Pineau and M. Javoy, *ibid.* **123**, 179 (1994).
 6. C. Allègre, T. Staudacher, P. Sarda, M. Kurz, *Nature Earth Planet. Sci. Lett.* **81**, 127 (1986/87).
 7. The stepwise crushing (five steps and eight steps) and the measurements on two different mass spectrometers (ARESIBO I and ARESIBO II) were performed as described in M. Moreira, T. Staudacher, P. Sarda, J.-G. Schilling, C. Allègre, *Earth Planet. Sci. Lett.* **133**, 367 (1995).
 8. T. Staudacher, M. Moreira, C. Allègre, *Mineral. Mag.* **58A**, 874 (1994); C. Allègre, M. Moreira, T. Staudacher, *Geophys. Res. Lett.* **22**, 2325 (1995).
 9. H. Craig and J. Lupton, *Earth Planet. Sci. Lett.* **31**, 369 (1976); I. Kaneoka and N. Takaoka, *ibid.* **39**, 382 (1978); M. Kurz, W. Jenkins, S. Hart, *Nature* **297**, 43 (1982); T. Staudacher, M. Kurz, C. J. Allègre, *Chem. Geol.* **56**, 193 (1986); T. Staudacher, P. Sarda, C. Allègre, *ibid.* **59**, 35 (1990).
 10. I. Yatssevich and M. Honda, *J. Geophys. Res.* **102**, 10291 (1997).
 11. Rare gases in the solar system can be—in a first-order approach—subdivided into planetary, as found in chondrites and the atmospheres of the inner planets, and solar, as ejected from the sun in the solar wind and flares and implanted in the surface of orbiting objects such as meteoroids and the moon. The isotopic composition of Ne is distinct for these components. Solar Ne has a $^{20}\text{Ne}/^{22}\text{Ne} = 13.8$ [J.-P. Benkert, H. Baur, P. Signer, R. Wieler, *J. Geophys. Res.* **98**, 13147 (1993)]. Planetary Ne is heavier, with $^{20}\text{Ne}/^{22}\text{Ne} = 8.5$ [E. Mazor, D. Heymann, E. Anders, *Geochim. Cosmochim. Acta*, **34**, 781 (1970)], though it might be better represented by "phase-Q Ne," with $^{20}\text{Ne}/^{22}\text{Ne} = 10.7$ (29).
 12. M. Honda, I. McDougall, D. Patterson, A. Dougeris, D. Clague, *Nature* **349**, 149 (1991).
 13. R. Poreda and K. Farley, *Earth Planet. Sci. Lett.* **113**, 129 (1992).
 14. M. Moreira, P. Valbracht, T. Staudacher, C. Allègre, *Geophys. Res. Lett.* **23**, 2453 (1996); P. Valbracht *et al.*, *Earth Planet. Sci. Lett.* **138**, 29 (1996).
 15. P. Valbracht, T. Staudacher, A. Malahoff, C. Allègre, *Earth Planet. Sci. Lett.* **150**, 399 (1997).
 16. M. Moreira and C. Allègre, *Chem. Geol.*, in press.
 17. We have considered maximum $^{20}\text{Ne}/^{22}\text{Ne}$ ratios measured by Sarda *et al.* (2); H. Hiyagon, M. Ozima, B. Marty, S. Zashu, H. Sakai, *Geochim. Cosmochim. Acta* **56**, 1301 (1992); and unpublished data from our laboratory. One point from (2) with a $^{20}\text{Ne}/^{22}\text{Ne}$ ratio of 13.2 ± 1.0 was not considered because of its large uncertainty.
 18. S. Niedermann, W. Bach, J. Erzinger, *Geochim. Cosmochim. Acta* **61**, 2697 (1997).
 19. M. Ozima, *Rev. Geophys.* **32**, 405 (1994).
 20. P. Burnard, D. Graham, G. Turner, *Science* **276**, 568 (1997).
 21. We can write the equation

$$\left[\frac{^{21}\text{Ne}}{^{22}\text{Ne}} \right]_{\text{MORB}} = \left[\frac{^{21}\text{Ne}}{^{22}\text{Ne}} \right]_i + \left[\frac{^{21}\text{Ne}^*}{^4\text{He}^*} \right] \left[\frac{^4\text{He}^*}{^3\text{He}} \right] \left[\frac{^3\text{He}}{^{22}\text{Ne}} \right]$$

where $(^{21}\text{Ne}/^{22}\text{Ne})_i$ is the initial ratio, $(^{21}\text{Ne}/^{22}\text{Ne})_{\text{MORB}}$ is the MORB ratio (actual), $(^{21}\text{Ne}^*/^4\text{He}^*)$ is the production ratio, and $(^4\text{He}^*/^3\text{He})$ is the difference between the MORB ratio ($\sim 90,000$) and the $^4\text{He}/^3\text{He}$ initial ratio [either 5000 (solar) or 20,000 (in the present lower mantle)]. If it is assumed that the upper mantle is a closed system (after the outgassing), $(^{21}\text{Ne}/^{22}\text{Ne})_i = 0.0328$ (solar), $(^{21}\text{Ne}/^{22}\text{Ne})_{\text{MORB}} = 0.075$, $(^{21}\text{Ne}^*/^4\text{He}^*) = 4.5 \times 10^{-8}$ (70) or 9×10^{-8} [T. Kyser and W. Rison, *J. Geophys. Res.* **87**, 5611 (1982)], and $(^4\text{He}^*/^3\text{He}) = 90,000 - 5000 = 85,000$, we can estimate that the $^3\text{He}/^{22}\text{Ne}$ ratio is between $11 (^{21}\text{Ne}^*/^4\text{He}^* = 4.5 \times 10^{-8})$ and $5.5 (^{21}\text{Ne}^*/^4\text{He}^* = 9 \times 10^{-8})$, a value that is very similar to our measurements. These results are exactly the same in the case of an upper mantle in a steady state [(22); K. O'Nions and I. Tolstikhin, *Earth Planet. Sci. Lett.* **124**,

131 (1994); L. Kellogg and G. Wasserburg, *Earth Planet. Sci. Lett.* **99**, 276 (1990)].
 22. D. Porcelli and G. Wasserburg, *Geochim. Cosmochim. Acta* **59**, 4921 (1995).
 23. B. Marty and P. Alle, in *Noble Gas Geochemistry and Cosmochemistry*, J. Matsuda, Ed. (Terra Scientific, Tokyo, 1994), pp. 191–204.
 24. C. Harper and S. Jacobsen, *Science* **273**, 1814 (1996).
 25. T. Owen, A. Bar-Nun, I. Kleinfeld, *Nature* **358**, 43 (1992).
 26. B. Marty, *Earth Planet. Sci. Lett.* **94**, 45 (1989).
 27. R. Pepin, *Icarus* **92**, 2 (1991).
 28. Review in M. Ozima and F. Podosek, *Noble Gas Geochemistry* (Cambridge Univ. Press, Cambridge, 1983), pp. 1–367; M. Ozima and K. Zahnle, *Geochim. J.* **27**, 185 (1993); I. Azbel and I. Tolstikhin, *Meteoritics* **28**, 609 (1993).
 29. The isotopic composition of stable isotopes of Kr and Xe in Earth's atmosphere is different from their solar and planetary isotopic compositions (28). Although the origin of this fractionation is still debated (27), it may indicate that the evolution of these isotopic ratios is even more complicated than for He, Ne, and Ar, and that Kr and Xe are rather unsuitable for testing our model. They would also fail to serve as a test because their solar and planetary compositions show quite similar isotopic patterns (28). Finally, there is to our knowledge no evidence that the composition of stable isotopes of Kr and Xe in the mantle differs from that in the atmosphere, which may indicate the injection of some atmospheric Kr and Xe into the mantle as may have also happened for Ne and would explain the lower-than-solar $^{20}\text{Ne}/^{22}\text{Ne}$ ratio in the upper mantle.
 30. R. Wieler, E. Anders, H. Baur, R. Lewis, P. Signer, *Geochim. Cosmochim. Acta* **55**, 1709 (1991).
 31. J. Yangang and E. Anders, *ibid.* **46**, 877 (1982); J. F. Wacker, *ibid.* **53**, 1421 (1989).
 32. F. Fanale and P. Cannon, *Earth Planet. Sci. Lett.* **11**, 361 (1971); F. A. Podosek, T. J. Bernatowicz, F. E. Kramer, *Geochim. Cosmochim. Acta* **45**, 2401 (1981).
 33. D. Hunten, R. Pepin, J. Walker, *Icarus*, **43**, 22 (1987).
 34. This is contribution number 1510 of the Institut de Physique du Globe de Paris. We thank P. Sarda, T. Staudacher, M. Javoy, F. Pineau, and P. Cartigny for discussions. The manuscript was improved by the comments of two anonymous reviewers.

27 October 1997; accepted 14 January 1998

The Formation of HCS and HCSH Molecules and Their Role in the Collision of Comet Shoemaker-Levy 9 with Jupiter

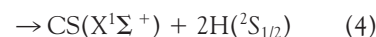
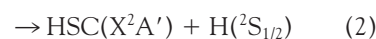
R. I. Kaiser,* C. Ochsenfeld, M. Head-Gordon, Y. T. Lee†

The reaction of hydrogen sulfide with ground-state atomic carbon was examined with crossed molecular beams experiments and ab initio calculations. The thiohydroxycarbene molecule, HCSH, was the reactive intermediate, which fragmented into atomic hydrogen and the thioformyl radical HCS. This finding may account for the unassigned HCS source and an unidentified HCSH radical needed to match observed CS abundances from the collision of comet Shoemaker-Levy 9 into Jupiter. In the shocked jovian atmosphere, HCS could further decompose to H and CS, and CS could react with SH and OH to yield the observed CS₂ and COS.

The discovery of comet D/Shoemaker-Levy 9 (SL9) initiated the only observation of the collision of two solar system bodies (1). From 16 to 22 July 1994, about 20 fragments of the split nucleus impacted into Jupiter causing enormous atmospheric disturbances (2, 3). Earth-based observations detected large amounts of the sulfur-containing molecules S₂, COS, CS₂, CS, and H₂S, which are not indigenous to Jupiter's atmosphere (4–6). Generic reaction networks simulating the impact-induced sulfur chemistry suffered from the lack of laboratory data on products and intermediates in

the H-C-S system and failed to quantitatively reproduce observed abundances of sulfur-containing species in Jupiter's atmosphere. To match the observed data qualitatively, impact models had to include postulated reactions involving transient species such as HCS and CH₂S in the form of thioformaldehyde (H₂CS) (7, 8).

We present crossed molecular beams experiments and ab initio calculations on the reaction of ground-state carbon atoms, C(³P₁), with hydrogen sulfide, H₂S:



Atomic carbon is formed in initial SL9 collision-triggered shock waves characterized by high temperature of up to 5000 K and might survive reentry of the impact

Department of Chemistry, University of California, Berkeley and Chemical Sciences Division, Lawrence Berkeley National Laboratory, Berkeley, CA 94720, USA.

*Present address: Academia Sinica, Institute of Atomic and Molecular Sciences, 1, Section 4, Roosevelt Road, Taipei, 116, Taiwan, Republic of China, and Department of Physics, Technical University Chemnitz-Zwickau, 09107 Chemnitz, Germany.

†Present address: Academia Sinica, Institute of Atomic and Molecular Sciences, 1, Section 4, Roosevelt Road, Taipei, 116, Taiwan, Republic of China.

plume (4, 5). Upon reaction of atomic carbon with hydrogen sulfide from either Jupiter or the SL9 fragments (9), the formation of organosulfur molecules is expected.

All ab initio calculations were performed to predict relative energies to an accuracy of 5 to 10 kJ mol⁻¹ (10). Singlet thioformaldehyde, H₂CS (7 in Fig. 1), is the global energy minimum on the CH₂S surface and is bound by 550.4 kJ mol⁻¹ with respect to the reactants (Fig. 1 and Table 1). Its singlet-triplet gap of 167.5 kJ mol⁻¹ agrees with recent results of spectroscopic investigations of 174 kJ mol⁻¹ (11). Singlet *trans*- and *cis*-thiohydroxycarbene {4}/5, HCSH, lie 184.8 kJ mol⁻¹ and 189.8 kJ mol⁻¹ above singlet thioformaldehyde. Triplet thiohydroxycarbene {3} is energetically less favored by 76.1 kJ mol⁻¹ compared with singlet *trans*-thiohydroxycarbene. Finally, triplet and singlet 2,2-dihydrothiocarbonyl {2}/1, H₂SC, are only 63.5 and 57.3 kJ mol⁻¹ more stable than the reactants. HSC is less stable by 165.6 kJ mol⁻¹ compared with HCS. The computed HCS enthalpy of formation of 296.2 kJ mol⁻¹ agrees with values from photoionization mass spectrometric studies [300.4 ± 8.4 kJ mol⁻¹ (12, 13)]. Reaction exothermicities to form HCS + H (reaction 1) and HSC + H (reaction 2) are computed to be 183.9 kJ mol⁻¹ and 18.3 kJ mol⁻¹, respectively.

We performed our experiments under single-collision conditions at collision energies of 16.7 and 42.8 kJ mol⁻¹ using a universal crossed molecular beams apparatus (14). The fourth harmonic of a neody-

mium-yttrium-aluminium-garnet laser was focused on a rotating carbon rod, and ablated carbon atoms were seeded into neon and helium carrier gas (15). The pulsed carbon beam crossed a H₂S beam at 90°. Time-of-flight (TOF) spectra and product angular distributions of reactively scattered products were recorded in the scattering plane at a mass-to-charge ratio (*m/e*) of 45 for HCS and HSC and a *m/e* of 44 for CS by using a quadrupole mass spectrometer with an electron-impact ionizer. For physical interpretation, results were transformed into the center-of-mass (CM) reference frame. We used a forward-convolution routine to yield angular flux distribution *T*(θ) and translational energy flux distribution *P*(*E*) in the CM frame (16).

The laboratory angular distributions and TOF spectra of the reactive scattering signal at *m/e* = 45 (HCS and HSC) are presented in Figs. 2 and 3. TOF spectra at *m/e* = 44 and 45 depict identical shapes, indicating that HCS⁺ fragments partly to CS⁺ in the electron-impact ionizer and that channels 3 and 4 to CS are closed. No radiative association to H₂CS isomers was observed. These results indicate that HCS and HSC can be formed in the plume chemistry of SL9 fragments during impact into Jupiter. We also examined the chemical dynamics of the reaction to unveil information on intermediate H₂CS complexes and product isomers using the translational energy *P*(*E*) and angular distributions *T*(θ). Both translational energy distributions peak at 70 and 50 kJ mol⁻¹ at our

higher and lower collision energies, respectively. The experimental high-energy cut-offs of 208 and 232 kJ mol⁻¹ agree with the sum of our ab initio reaction energy for the HCS isomer and the relative collision energies, that is, 201 and 226 kJ mol⁻¹. The less stable HSC is expected to show cut-offs at 35 and 61 kJ mol⁻¹ and can be excluded as a major contribution to our signal (17). The shapes of the angular distributions (Fig. 4) depend on the collision energy *E_c*. As *E_c* increases from 16.7 to 42.8 kJ mol⁻¹, *T*(θ) changes from forward-backward symmetric to more forward-scattered. This suggests one reaction channel following indirect reactive scattering dynamics through a complex formation. At lower collision energy, the fragmenting H₂CS complex has a life-

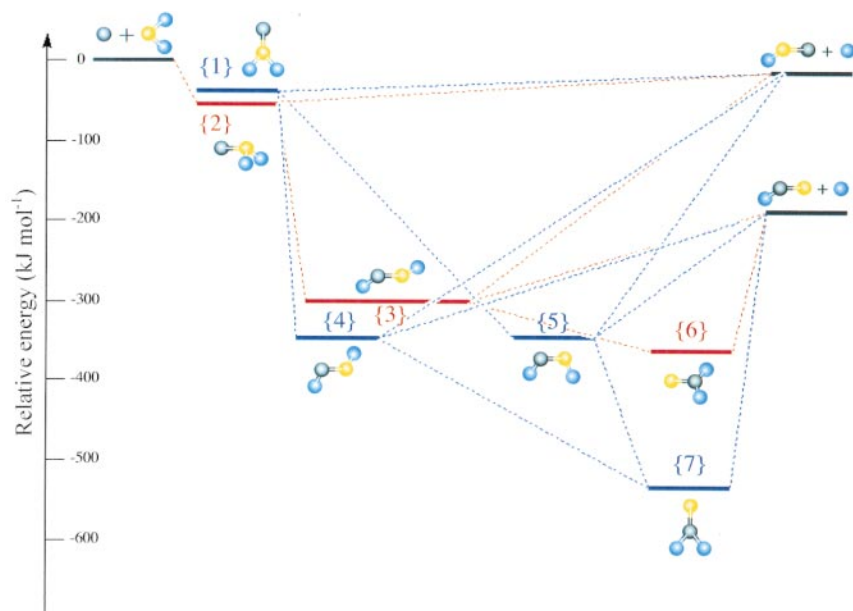


Fig. 1. Energy level diagram of the C(³P) + H₂S(X¹A₁) reaction and ab initio structures of H₂CS and HCS isomers. Red lines, singlet surface; blue lines, triplet surface. Gray balls denote carbon, blue balls hydrogen, and yellow balls sulfur. Solid black lines define local minima, hereafter designated in curly brackets, whereas dashed lines show potential reaction pathways.

Table 1. Structural data and rotational constants (A, B, and C) of H₂CS isomers as shown in Fig. 1 and HCS/HSC. Notation: (S-C) = 162.2 denotes bond length in picometers (S,C,H) = 122.0° denotes bond angle with apical atom C, (S,H,H,C) = 20.3° stands for the out-of-plane angle between the bond S-C and the plane H-H-C, and (H-C-S-H) = 97.2° stands for the torsion angle H-C-S-H. Pt. group, point group.

Isomer (Pt. group)	Structural data	A, B, C (cm ⁻¹)
¹ H ₂ CS (C _{2v})	(S-C) = 162.2 (C-H) = 108.8 (S,C,H) = 122.0°	A = 9.840 B = 0.583 C = 0.550
³ H ₂ CS (C _s)	(S-C) = 171.5 (C-H) = 108.2 (S,C,H) = 118.3° (S,H,H,C) = 20.3°	A = 9.295 B = 0.532 C = 0.505
¹ HCSH _{trans} (C _s)	(H-C) = 110.8 (C-S) = 168.3 (S-H) = 135.4 (H,C,S) = 100.8° (C,S,H) = 99.6°	A = 6.164 B = 0.613 C = 0.558
¹ HCSH _{cis} (C _s)	(H-C) = 110.0 (C-S) = 166.2 (S-H) = 137.7 (H,C,S) = 109.5° (C,S,H) = 109.4°	A = 6.347 B = 0.615 C = 0.560
³ HCSH (C ₁)	(H-C) = 108.4 (C-S) = 171.7 (S-H) = 135.3 (H,C,S) = 129.6° (C,S,H) = 98.5° (H-C-S-H) = 97.2°	A = 7.251 B = 0.550 C = 0.530
¹ H ₂ SC (C _{2v})	(C-S) = 160.8 (S-H) = 139.6 (C,S,H) = 132.1°	A = 7.787 B = 0.643 C = 0.594
³ H ₂ SC (C _s)	(C-S) = 196.5 (S-H) = 135.4 (C,S,H) = 104.6° (C,H,H,S) = 68.7°	A = 5.067 B = 0.460 C = 0.454
HCS (C _s)	(H-C) = 108.7 (C-S) = 156.4 (H,C,S) = 132.3°	A = 30.783 B = 0.678 C = 0.663
HSC (C _s)	(H-S) = 136.7 (S-C) = 165.6 (H,S,C) = 102.7°	A = 9.858 B = 0.687 C = 0.642

time longer than its rotational period, but with increasing collision energy (18), the lifetime of the complex is reduced to less than one rotational period.

We have tried to classify the fragmenting H_2CS complex or complexes. The identification of HCS excludes decomposing singlet or triplet H_2SC {1}/{2}, because S–H bond rupture would yield HSC. Furthermore, $T(\theta)$ shows forward peaking at higher collision energy. This requires that the incorporated C and the escaping H atom must be located on opposite sites of the rotational axes. On the basis of our ab initio geometries of H_2CS {6}/{7}, no rotation axis fulfills this requirement. Hence, thioformaldehyde can be excluded as the decomposing complex. Therefore, thiohydroxycarbenes {3}, {4}, and {5} are the only remaining intermediates. Each can rotate around the B/C axis to account for the forward-peaked $T(\theta)$, yielding HCS and H in the final bond rupture about 0.1 ps after HCSH formation (18, 19).

We identified the thioformyl radical, HCS, as the major product of $\text{C} + \text{H}_2\text{S}$ under single-collision laboratory condi-

tions. This reaction may account for the unassigned HCS source required for chemical reaction networks to match observed CS abundances in the impact plumes from the collision of SL9 fragments into Jupiter. At 5000 K, where chemical models predict atomic carbon to be present during the initial impact (8, 9), the most probable translation energy is about 50 kJ mol^{-1} , close to our collision energy of 42.8 kJ mol^{-1}

mol^{-1} . The high-energy tail of the Maxwell-Boltzman distribution could enable HCS to be formed with more internal energy to undergo secondary decomposition to CS and H in the jovian atmosphere. CS might react with SH or OH to form observed CS_2 and COS (4, 5). Also, our investigations classify a thiohydroxycarbene complex, HCSH, as the reaction intermediate to form HCS and H. Although its lifetime is too short to survive under our single-collision conditions, the denser jovian atmosphere could allow a three-body collision. In this way internal energy can be diverted, thus stabilizing HCSH. HCSH should be included in impact models to account for observed jovian CS abundances, whereas only the thioformaldehyde molecule has been incorporated so far (7).

Our results help to unravel the complex impact-induced chemistry that occurred during collision of SL9 with Jupiter. We have suggested some formation mechanisms of CS, CS_2 , and COS and have documented the role of transient species HCS and HCSH. However, compared with our experiments, many complications exist in the real jovian system. First, C atoms might react concurrently with other molecules such as acetylene, ethene, and hydrogen cyanide (20); even formation of CH_2 through a three-body reaction with H_2 is energetically feasible. Second, other pathways could contribute to H_2CS and HCS: HCS may be produced through reaction of S atoms with CH_3 radicals (7), initially forming H and H_2CS . The H_2CS could be photolyzed, yielding HCS and H, which could then form CS and CS_2 by photochemical reactions (21). Third, molecules formed during the initial, high-energy explosion might be altered as the impact plume reenters the jovian atmosphere. The fraction of molecules that survive the plume reentry has not been established yet, but these multiple shock events are important for the final state of the gas. This reentry shock is characterized by moderate temperatures [500 to 2500 K (22)], and the significance of atomic carbon under these conditions has not yet been determined. The complexity of this planetary system makes it difficult to define the most important reaction contributing to the SL9 impact-induced sulfur chemistry and to model different reactions at distinct stages of the impact process simultaneously.

REFERENCES AND NOTES

1. C. S. Shoemaker, E. M. Shoemaker, D. Levy, *Int. Astron. Union Circ.* 5725 (1993).
2. K. S. Noll, H. A. Weaver, P. D. Feldman, Eds., *The Collision of Comet Shoemaker-Levy 9 and Jupiter* (Cambridge Univ. Press, Cambridge, 1996).
3. J. Crovisier, in (2), pp. 31–50.
4. S. K. Atreya et al., *Geophys. Res. Lett.* 22, 1625

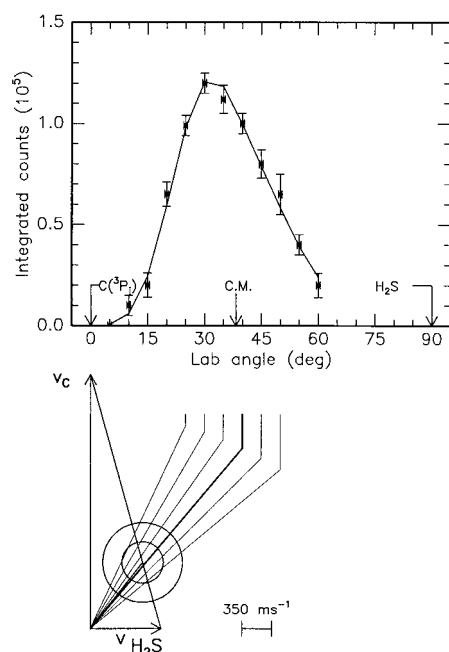


Fig. 2. (Top) HCS product laboratory angular distribution of the reaction $\text{C}(^3\text{P}) + \text{H}_2\text{S}(X^1\text{A}_1)$ at a collision energy of 42.8 kJ mol^{-1} . Filled circles and 1σ error bars indicate experimental data, solid lines are the calculated distributions, and C.M. indicates the center-of-mass angle. (Bottom) Corresponding velocity vector diagram. v_C and $v_{\text{H}_2\text{S}}$ indicate velocities of C and H_2S beams in the laboratory frame. The inner circle represents the maximum CM recoil velocity of HSC, the outer circle for HCS, assuming all available energy channels into translational energy of the products. The solid lines point to distinct laboratory angles whose TOFs are shown in Fig. 3.

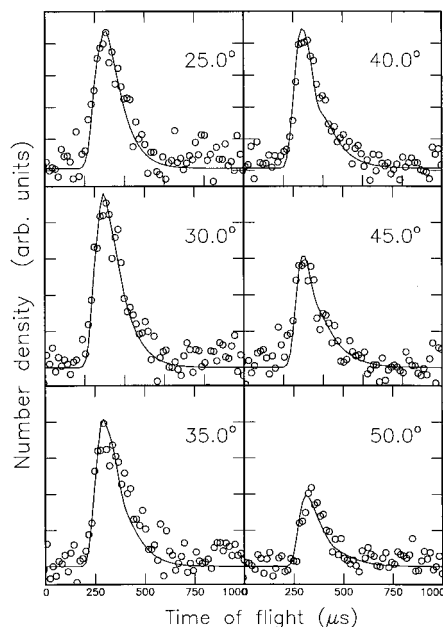


Fig. 3. Normalized TOF data of HCS at $m/e = 45$ at 42.8 kJ mol^{-1} collision energy. Open circles represent experimental data, and the solid line the fit. Arb. units, arbitrary units.

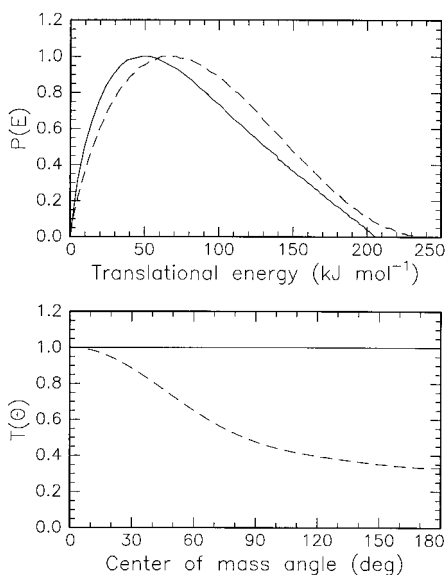


Fig. 4. CM angular flux distributions $T(\theta)$ (bottom) and translational energy flux distributions $P(E)$ (top) for $\text{C}(^3\text{P}) + \text{H}_2\text{S}(X^1\text{A}_1)$ at peak collision energies of 16.7 (solid lines) and 42.8 kJ mol^{-1} (dashed line).

- (1995); R. V. Yelle and M. A. McGrath, *Icarus* **119**, 90 (1996); E. Leloch, in (2), pp. 213–242; E. Leloch et al., *Nature* **373**, 592 (1995).
- K. S. Noll et al., *Science* **267**, 1307 (1995). The Galileo Probe mass spectrometer identified H₂S in Jupiter's atmosphere (23).
 - S. Atreya et al., in *Three Galileos: The Man, the Spacecraft, the Telescope*, J. Rahe et al., Eds. (Kluwer, Dordrecht, in press).
 - K. Zahnle et al., *Geophys. Res. Lett.* **22**, 1593 (1995); K. Zahnle in (2), pp. 183–212.
 - S. Borunov, P. Drossart, T. Encrenaz, V. Dorofeeva, *Icarus* **125**, 121 (1997).
 - There are four possible sources of H₂S for the reaction. First, impact models for the period immediately after the high-temperature explosion agree on formation of H₂S and atomic carbon (7, 8). Second, H₂S from the comet itself might have survived in the outer, less energized regions of the impact plume (3). Third, models of the jovian cloud structure predict ammonium hydroxysulfide (NH₄HS) clouds [S. K. Atreya and P. N. Romani, in *Planetary Meteorology*, G. E. Hund, Ed. (Cambridge Univ. Press, Cambridge, 1985)]. The Galileo probe nephelometer indicated tenuous clouds [B. Regent, D. S. Colburn, P. Aurin, K. A. Rages, *Science* **272**, 854 (1996)], presumably composed of NH₄HS [(7); S. Atreya, private communication]. If shock waves reached these layers, reaction to ammonia, NH₃, and H₂S may have occurred [S. K. Atreya, *Atmospheres and Ionospheres of the Outer Planets and Their Satellites* (Springer, Berlin, 1986)]. And fourth, H₂S was identified in the jovian atmosphere by the Galileo probe mass spectrometer (7, 23).
 - Calculations used unrestricted CCSD(T) [K. Raghavachari, G. W. Trucks, J. A. Pople, M. Head-Gordon, *Chem. Phys. Lett.* **157**, 479 (1989)] in ACES II [J. F. Stanton, J. Gauss, J. D. Watts, W. J. Lauderdale, R. J. Bartlett, *Int. J. Quantum Chem. Symp.* **26**, 879 (1992)]. Triple zeta polarization (TZP) basis sets for H₂CS isomers and quadruple zeta double polarization (QZPP) [A. Schäfer, H. Horn, R. Ahlrichs, *J. Chem. Phys.* **97**, 2571 (1992)] for HCS and HSC were used for structure optimization and frequencies. Relative energies for H₂CS isomers and HCS and HSC were calculated with QZPP and QZ triple polarization (QZ3P), respectively. QZ3P used Dunning's exponents [T. H. Dunning, *ibid.* **90**, 1007 (1989)].
 - R. H. Judge, D. C. Moule, G. W. King, *J. Mol. Spectrosc.* **81**, 37 (1980); M. R. J. Hachey and F. Grein, *Chem. Phys.* **197**, 61 (1995).
 - Enthalpies of formation $\Delta H_{F^{\circ}(HCS)}$ are calculated as follows: $\Delta H_{F^{\circ}} = \Delta H_{F^{\circ}(HCS)} + \Delta H_{F^{\circ}(H)} - \Delta H_{F^{\circ}(H_2S)} - \Delta H_{F^{\circ}(C)}$.
 - B. Ruscic and J. Berkowitz, *J. Chem. Phys.* **98**, 2568 (1993).
 - Y. T. Lee, *Science* **236**, 793 (1987). Peak velocities of carbon beams were determined to be 2980 and 1730 ms⁻¹, and those of the H₂S beams were 830 and 880 ms⁻¹.
 - R. I. Kaiser and A. G. Suits, *Rev. Sci. Instrum.* **66**, 5405 (1995).
 - E. A. Entenmann, thesis, Harvard University, Cambridge, MA (1966).
 - Upper limits of HSC are 10%.
 - W. B. Miller, thesis, Harvard University, Cambridge, MA (1969). The rotational period of the decomposing H₂CS acts as a clock in the experiment to estimate its lifetime.
 - The dynamics leading to the thiohydroxycarbene are governed by the addition of C(³P₁) to H₂S to form {2}. Direct insertion into the S–H bond of H₂S to yield triplet {3} is symmetry forbidden and should have an entrance barrier larger than our lowest collision energy. The S atom and narrow 6.2 kJ mol⁻¹ singlet-triplet gap of {1} and {2} could induce intersystem crossing (ISC) followed by H migration to {4}/5. Alternatively, {2} could undergo H migration to {3} and ISC to {4}/5.
 - R. I. Kaiser, C. Ochsenfeld, M. Head-Gordon, Y. T. Lee, A. G. Suits, *Science* **274**, 1508 (1996).
 - J. Moses, in (2), p. 243.
 - B. J. Conrath, in (2), pp. 293–307.

- H. B. Niemann et al., *Science* **272**, 846 (1996).
- R.I.K. and C.O. thank the Deutsche Forschungsgemeinschaft (DFG) for Habilitation and postdoctoral fellowships, respectively. R.I.K. further thanks D. Gerlich and Y.T.L. for support. M.H.G. acknowledges a Packard fellowship. We acknowledge useful

comments from S. K. Atreya, J. F. Stanton, and P. Casavecchia and discussions with M. F. A'Hearn and K. S. Noll. This work was supported by the U.S. Department of Energy.

30 October 1997; accepted 15 January 1998

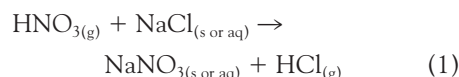
Direct Observation of Heterogeneous Chemistry in the Atmosphere

Eric E. Gard, Michael J. Kleeman, Deborah S. Gross, Lara S. Hughes, Jonathan O. Allen, Bradley D. Morrical, David P. Fergenson, Tas Dienes, Markus E. Gälli, Robert J. Johnson, Glen R. Cass,* Kimberly A. Prather*

The heterogeneous replacement of chloride by nitrate in individual sea-salt particles was monitored continuously over time in the troposphere with the use of aerosol time-of-flight mass spectrometry. Modeling calculations show that the observed chloride displacement process is consistent with a heterogeneous chemical reaction between sea-salt particles and gas-phase nitric acid, leading to sodium nitrate production in the particle phase accompanied by liberation of gaseous HCl from the particles. Such single-particle measurements, combined with a single-particle model, make it possible to monitor and explain heterogeneous gas/particle chemistry as it occurs in the atmosphere.

Airborne particles have an important influence on Earth's radiation balance that can lead to climate forcing (1). In addition, they are responsible for much of the visibility reduction observed in urban areas and national parks (2) and can adversely affect human health (3). These particles are introduced directly into the atmosphere from natural activities (for example, sea spray and volcanic eruptions) and anthropogenic pollution sources. As they evolve in the atmosphere, their chemical and physical properties—and hence their characteristics, such as light scattering and toxicity—change by accumulation of atmospheric gas-phase chemical reaction products or through heterogeneous reactions with gas-phase species. For example, gaseous sulfur dioxide emitted from fossil fuel combustion, as well as organic species emitted from both anthropogenic and biogenic sources, can react in the atmosphere to form particulate sulfates (4) or secondary organic aerosols (5), respectively. Additionally, gas-phase emissions of nitrogen oxides from combustion sources undergo homogeneous atmospheric reactions to produce gaseous species

including N₂O₅ and HNO₃ (6, 7). These gases can diffuse to the surface of sea-salt particles where heterogeneous reactions can lead to chloride displacement from sodium chloride-containing particles, for example, by



(subscripts g, s, and aq refer to gaseous, solid, and aqueous phase species, respectively), leaving sodium nitrate in the particle phase (8).

In order to assess the effect of airborne particles on atmospheric processes, the primary particle emissions, secondary particle formation processes, and relevant heterogeneous chemistry must be understood theoretically and confirmed experimentally. The reactant-product relations involved in the heterogeneous chemistry of aerosols are generally inferred from bulk samples of atmospheric particles collected on filters or on cascade impactor substrates. Unfortunately, atmospheric particulate matter is a complex mixture of particles of many different sizes and chemical compositions, and therefore, the exact chemical speciation of the individual particles cannot be determined by bulk filter analysis. For example, if sulfate, nitrate, sodium, and ammonium ions are all present in a bulk sample, one cannot distinguish whether all particles contain each chemical species or whether pure ammonium sulfate particles coexist with pure sodium nitrate particles in the same air mass.

E. E. Gard, D. S. Gross, B. D. Morrical, D. P. Fergenson, T. Dienes, M. E. Gälli, K. A. Prather, Department of Chemistry, University of California, Riverside, CA 92521, USA.

M. J. Kleeman, L. S. Hughes, J. O. Allen, R. J. Johnson, G. R. Cass, Department of Environmental Engineering Science, California Institute of Technology, Pasadena, CA 91125, USA.

*To whom correspondence should be addressed. E-mail: glen@eql.caltech.edu; prather@citrus.ucr.edu